Available online at www.sciencedirect.com
SCIENCE DIRECT®

Journal of the European Ceramic Society 24 (2004) 847–854

www.elsevier.com/locate/jeurceramsoc

# Thermal shock behaviors of functionally graded ceramic tool materials

Jun Zhao*, Xing Ai, Jianxin Deng, Jinghai Wang

*School of Mechanical Engineering, Shandong University, Jinan 250061, PR China*

Received 29 January 2003; received in revised form 4 April 2003; accepted 27 April 2003

**Abstract**

Thermal shock resistance of $Al_2O_3$–TiC and $Al_2O_3$–(W, Ti)C functionally graded ceramic tool materials with symmetrical structures were evaluated by water quenching and subsequent three-point bending tests of strength diminution. Comparisons were made with the results from parallel experiments conducted using homogeneous $Al_2O_3$–TiC and $Al_2O_3$–(W, Ti)C ceramic tool materials. Functionally graded cutting ceramics exhibited both increased critical temperature difference and increased strength retention properties compared to homogeneous cutting ceramics, indicating their higher thermal shock resistance. The experimental results were discussed and rationalized in terms of microstructural observations and the calculations of one-dimensional transient temperature fields and transient thermal stress fields in case of surface cooling by using the perturbation method. It was concluded that higher thermal shock resistance could be achieved by means of varying the compositional distribution and hence the resultant distribution of thermo-mechanical properties of ceramic tool materials appropriately.


*Keywords:* $Al_2O_3$–TiC; Cutting tools; Functionally graded materials; Thermal shock resistance

## 1. Introduction

Engineering ceramics, by virtue of higher melting point, hardness, wear resistance and chemical stability as well as recent improvements in strength, toughness and fatigue resistance, have found their more and more applications as cutting tools in high speed machining and in the machining of difficult-to-cut materials. Despite some advantages, ceramic tool materials especially $Al_2O_3$-based ceramics always have greater thermal shock sensitivity than cemented carbide tools, because of an unfavorable ratio of stiffness and thermal expansion to strength and thermal diffusivity, and their limited plastic deformation. Due to the lower thermal conductivity, severe temperature grades and thermal stress grades are present in the interior of the ceramic cutting tool under cyclic mechanical and thermal shock in an intermittent cutting process, which may lead to the nucleation and growth of cracks and ultimately the fracture of the cutting edge. Unpredictable failure by fracture can lead to damage to the part being machined or to the machine tool, both of which can be several orders of magnitude more valuable than the tool itself in modern industry with the increased use of CNC (computerized numerical control) machine tools. Previous work on the thermal shock behavior of $Al_2O_3$-based ceramics has focused on the development of internal stresses due to thermal expansion mismatch, i.e. by increasing flaw tolerance, as indicated by pronounced *R*-curve behavior.[1] This is considered one of the processing strategies to increase thermal shock resistance of $Al_2O_3$-based ceramics.

In the present work we present a new approach to improving the thermal and mechanical properties especially the thermal shock resistance of $Al_2O_3$-based ceramic tool materials by introducing the concept of functionally graded materials (FGM).[2,3] If we design and fabricate the ceramic tool material with compositional distribution, microstructure varying continuously along the thickness direction in an optimum way to achieve the improved thermal and mechanical properties especially thermal shock resistance, it is expected to relax the temperature grades and thermal stress grades in the interior of the ceramic tool and hence to improve the fracture resistance especially the thermal fracture

* Corresponding author.
*E-mail address:* zhaojun@sdu.edu.cn (J. Zhao).

0955-2219/03/$ - see front matter © 2003 Elsevier Ltd. All rights reserved.
doi:10.1016/S0955-2219(03)00315-7

resistance of ceramic tool materials so as to meet the critical requirements of cutting process.

The present work was undertaken to evaluate the thermal shock behavior of $Al_2O_3$–TiC and $Al_2O_3$–(W, Ti)C functionally graded ceramic tool materials with symmetrical structures by using water quenching and subsequent three-point bending tests of strength diminution. Parallel experiments were conducted with reference homogeneous $Al_2O_3$–TiC and $Al_2O_3$–(W, Ti)C ceramics, respectively. The experimental results were discussed and rationalized in terms of microstructural observations and the calculations of one-dimensional transient temperature fields and transient thermal stress fields in case of surface cooling by using the perturbation method. Specifically, the effects of compositional distribution on thermal shock behavior of functionally graded ceramics were examined.

## 2. Materials and experimental procedures

An $Al_2O_3$–$X$ functionally graded ceramic tool material with $2m+1$ layers is assumed to have a symmetrical compositional distribution, where $X$ represents TiC or (W, Ti)C. (W, Ti)C is a solid solution composed of WC and TiC. Data of the physical properties of $\alpha$-$Al_2O_3$, TiC and (W,Ti)C are listed in Table 1. By not taking into account pores and other very small amounts of additives, the volume fraction of $X$ along the thickness direction is of the following exponential form[2, 3] (Fig. 1):

$$\phi_X(\bar{z}) = \begin{cases} (\phi_1 - \phi_m)(-\bar{z})^n + \phi_m & -1 \leqslant \bar{z} \leqslant 0 \\ (\phi_1 - \varphi_m)\bar{z}^n + \phi_m & 0 \leqslant \bar{z} \leqslant 1 \end{cases} \quad (1)$$

where $\bar{z}$ is a dimensionless coordinate variable in the thickness direction, $n$ is the distribution exponent which determine the compositional distribution of the material, $\phi_1$ and $\phi_m$ are volume fractions of $X$ of the two surface layers and the middle layer respectively.

If the volume fraction of $X$ in the $i$th layer is $\phi_i$, then the following relation is satisfied:

$$\phi_i = \phi_{2m-i} \; i = 1, 2, \cdots, 2m-1 \quad (2)$$

As shown in Fig. 1, the horizontal dashed lines representing the volume fractions $\phi_i$ of $X$ intersect a compositional distribution curve at different points $D_i$ which are then projected to the $\bar{z}$ axis to get a series of points $A_i$. The points $B_i$ used to determine the thickness of each layer $\overline{B_iB_{i+1}}$ are located according to the following relation:

$$\left.\begin{aligned} &\overline{A_{i-1}B_i} = \overline{B_iA_i} \qquad i = 2, 3, \cdots, 2m-1 \\ &\overline{B_1A_1} = \overline{A_1B_2} = \overline{B_{2m-1}A_{2m-1}} = \overline{A_{2m-1}B_{2m}} \end{aligned}\right\} \quad (3)$$

Then the final dimensionless thickness of each layer $h_i$ is given as:

$$h_i = \overline{B_iB_{i+1}} / \left(1 + 2\overline{B_1A_1}\right) \; i = 1, 2, \cdots, 2m-1 \quad (4)$$

Five different volume fractions of TiC (30, 40, 50, 60, 70 vol.%) were selected in designing the $Al_2O_3$–TiC functionally graded ceramic tool material with a nine-layer structure, with the volume fractions of TiC in the middle layer and surface layers being 30 and 70 vol.%, respectively. While in designing the $Al_2O_3$–(W, Ti)C functionally graded ceramic tool material with a seven-layer structure, four different volume fractions of (W, Ti)C (30, 35, 40, 45 vol.%) were selected, with the volume fractions of (W, Ti)C in the middle layer and surface layers being 30 and 45 vol.%, respectively. So for both $Al_2O_3$–TiC and $Al_2O_3$–(W, Ti)C functionally graded ceramics, the thermal expansion coefficient of the material increases from the surface to the middle position continuously (referring to Table 1). This may lead to the formation of residual compressive stresses in the surface region of the compact during the fabricating process (cooling from the sintering temperature to room temperature), which is favorable for an insert made of this kind of materials to resist external loading in cutting process.

The optimum distribution exponent $n=1.2$ was determined with the aim of the highest structural integrity of the compact i.e. the lowest residual thermal stress (Von Mises stress calculated by means of finite element method using a disc-shaped model shown in Fig. 2) in fabricating process.[3] Both the two surfaces of the compact can be used as rake faces of a cutting insert (Fig. 2). For $Al_2O_3$–TiC functionally graded ceramics with nine layers, the maximum residual radial compressive stress $\sigma_{rrmin}$ in the surface region is 271.6 MPa (absolute

Table 1
Data of the physical properties of $Al_2O_3$, TiC and (W, Ti)C

| Materials | Density ($\rho$/gcm$^{-3}$) | Thermal conductivity (20 °C) k/W(mK)$^{-1}$ | Specific heat (20 °C) c/J(gK)$^{-1}$ | Thermal expansion coefficient (20 °C) $\alpha$/10$^{-6}$K$^{-1}$ | Young's modulus (E/GPa) | Poisson's ratio $\nu$ |
|---|---|---|---|---|---|---|
| $\alpha$-$Al_2O_3$ | 3.99 | 40.37 | 0.774 | 8.5 | 380 | 0.26 |
| TiC | 4.93 | 24.28 | 0.561 | 7.6 | 450 | 0.19 |
| (W, Ti)C | 9.56 | 26.74 | 0.297 | 5.8 | 550 | 0.194 |

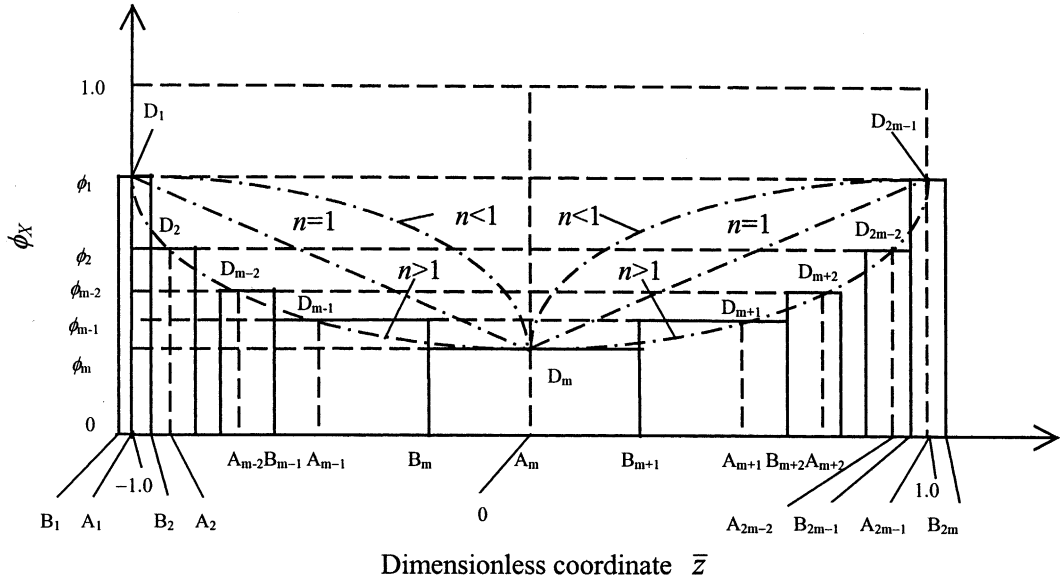


Fig. 1. Symmetrical composition distribution.

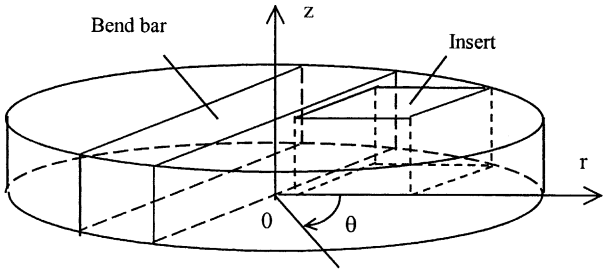


Fig. 2. Disc-shaped compact and sample/insert preparation.

value), the maximum residual radial tensile stress $\sigma_{rrmax}$ in the middle region is 244 MPa in the case of cooling from the sintering temperature 1700 °C to room temperature 20 °C.[3]

The starting materials were α-$Al_2O_3$ powder with average grain size of approximately 0.5 μm, purity 99.9%, and TiC powder with average grain size of 1.0 μm, purity 99.8% as well as (W, Ti)C powder with average grain size of 1.0 μm, purity 99.9%. Five $Al_2O_3$–TiC composite powders of different mixture ratios were prepared with the addition of the sintering additives MgO and $Y_2O_3$ in very small amounts (both 0.5 vol.%), and then laminated into the mould according to the predetermined compositional distribution. The sample with nine layers was then hot-pressed in flowing nitrogen for 20 min at 1700 °C temperature and 30 MPa pressure. This material was named FG-1. The $Al_2O_3$–(W, Ti)C functionally graded ceramic tool material with seven layers was synthesized by using the same techniques as described above and named FG-2.

Besides the functionally graded ceramics FG-1 and FG-2, a homogeneous $Al_2O_3$–TiC ceramics (30 vol.%$Al_2O_3$ + 70 vol.%TiC) and a homogeneous $Al_2O_3$–(W, Ti)C ceramics (55 vol.%$Al_2O_3$ + 45 vol.%(W, Ti)C) were synthesized for comparisons by using the same techniques.

Sintered specimens were cut and machined into bend bars for strength measurements as shown in Fig. 2. All specimen surfaces were ground flat to a 10 μm finish. Flexural strength was measured using a three-point bend fixture with a 30 mm span width at a loading crosshead rate of 0.5 mm/min, the surface perpendicular to the hot-pressing direction selected as the tensile (and compressive) surface. Measurements were performed on at least five test bars of each materials.

Bend bars were heated to desired temperature for 20 min in a furnace and then quenched into a container of water at 20 °C. Thermal quenching was conducted at temperatures 200 °C, 250, 300, 400, 600, 800 and 1000 °C. The shocked specimens were dried before retained strength was measured.

## 3. Results and discussion

### 3.1. Retained flexural strength

The variations of retained flexural strength of functionally graded ceramics and homogeneous ceramics with temperature difference are shown in Fig. 3. As shown in Fig. 3a, the retained flexural strength of quenched bars of FG-1 are more or less higher than those of $Al_2O_3$–TiC at all thermal shock temperature differences. The two materials exhibit different strength degradation behaviors. The strength of $Al_2O_3$–TiC remains approximately constant up to 230 °C and then drops precipitously in a range of temperature difference from 230 to 280 °C followed by moderate strength

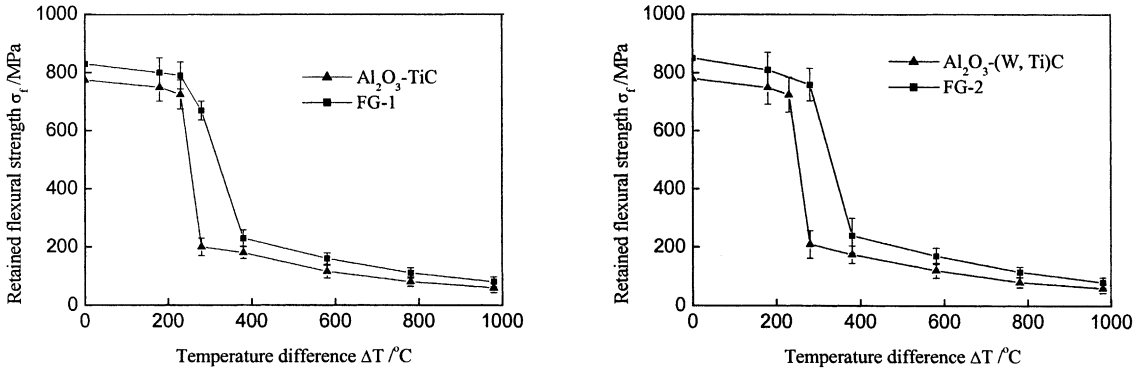


(a) FG-1 and homogeneous $Al_2O_3$-TiC ceramics (b) FG-2 and homogeneous $Al_2O_3$-(W,Ti)C ceramics

Fig. 3. Retained flexural strength versus temperature difference.

degradation. Whereas FG-1 exhibits an increased critical temperature difference for strength degradation compared to $Al_2O_3$–TiC, indicating higher thermal shock resistance.

Likewise, the functionally graded ceramics FG-2 shows a greater resistance to thermal shock than that of the homogeneous $Al_2O_3$–(W, Ti)C ceramics, in terms of both the increased critical temperature difference and the increased strength retention properties as shown in Fig. 3(b).

### 3.2. Microstructural features

No macroscopic crack was observed on quenched bars of all the four ceramics cooled from 200 and 250 °C, with the surfaces exhibiting a slight blue color. As the temperature difference increased to 280 °C, macro cracks formed on surfaces of homogeneous $Al_2O_3$–TiC and $Al_2O_3$–(W, Ti)C ceramics (Fig. 4), whereas few macro crack observed on surfaces of FG-1 and FG-2.

With the further increase of temperature difference, thin yellow oxide films formed on all the four ceramics. When the temperature difference increases higher than 780 °C, thick brown oxide layers formed on the specimen surfaces of all the four ceramics accompanied with peeling as shown in Fig. 5(a). Due to the thick oxide layers on the surfaces of quenched bars, macro cracks can not be observed easily. However, micro cracks are usually observed in the peeling areas [Fig. 5(a)], where the grains are elongated during the severe thermal shock [Fig. 5(b)].

Fig. 6 shows a ground sectional surface of FG-1 specimen quenched from 1000 °C, in which the symmetrically multi-layered structure and kinked cracks creating a closed region in the middle of the surface are clearly observed. Because of the complexity of thermal shock induced failure for functionally graded ceramics, the mechanisms of the crack nucleation, growth, branching and interlinking needs future investigations.

### 3.3. Calculations of transient thermal stresses

Because there are few thermal stress fracture resistance parameters suitable for the thermal shock resistance evaluation of functionally graded ceramics, the thermal shock response of the functionally graded ceramics can be investigated by means of the calculation of transient temperature fields and transient thermal

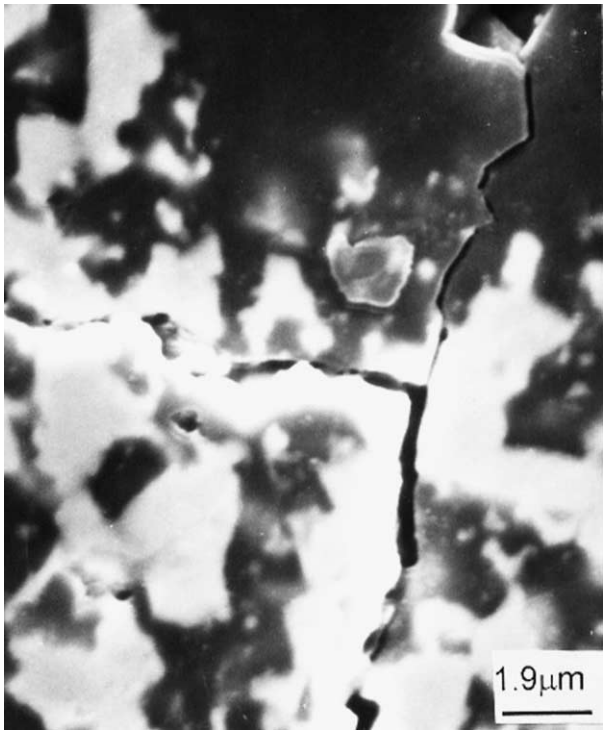


Fig. 4. Thermal shock induced cracking for $Al_2O_3$–(W,Ti)C under $\Delta T = 280$ °C.

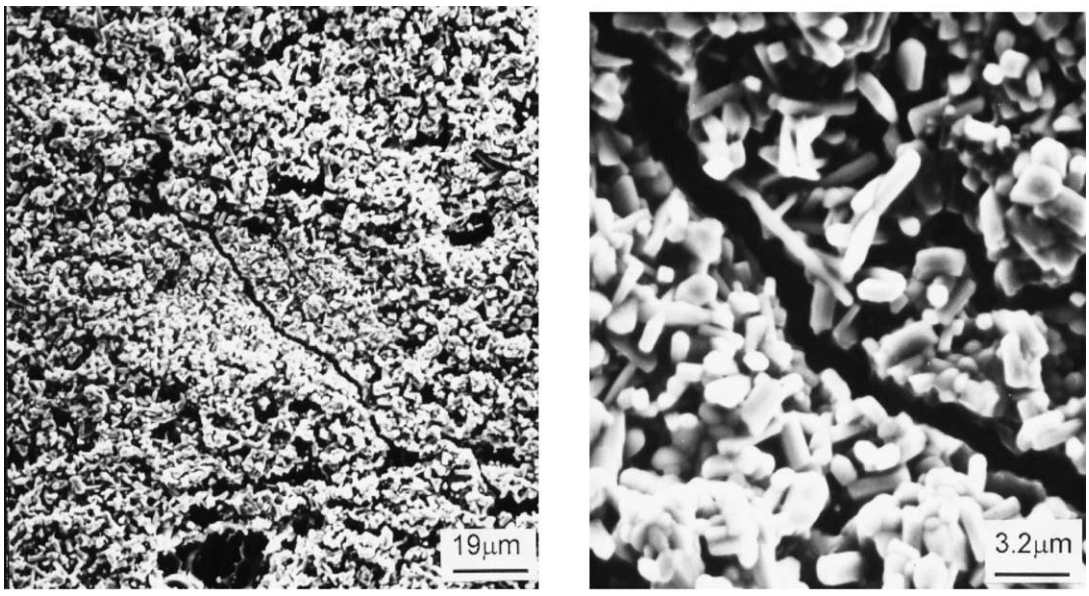


Fig. 5. Surface of FG-2 quenched from 1000 °C.

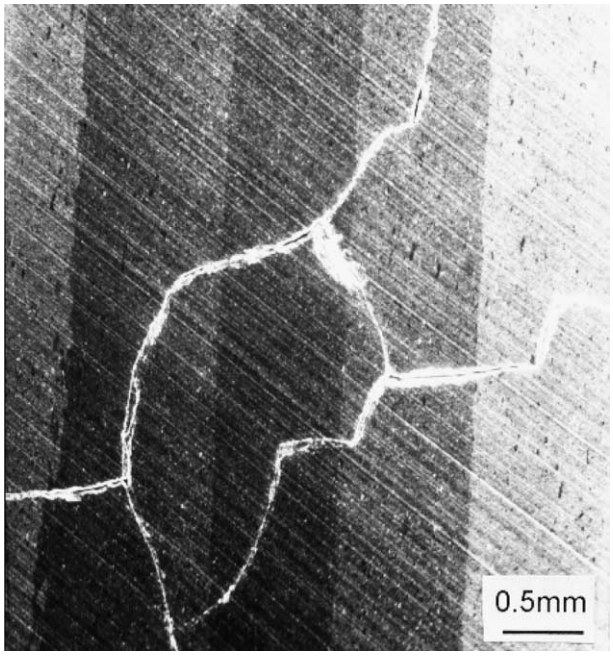


Fig. 6. Sectional surface of FG-1 quenched from 1000 °C.

stress fields, comparatively with that of homogeneous ceramics.

Without loss of universality, the calculations are carried out by using an infinite functionally graded ceramic plate with continuously graded composition rather than a discrete composition, with its thickness being $2r_m$ as shown in Fig. 7(a). It is assumed that initially the medium is at the uniform temperature $T_0$ and is suddenly subjected to an uniform temperature $T_s$ by the surrounding medium, only an idealized thermal shock condition considered, i.e. the heat transfer coefficient on the two surfaces being infinitely large. Because of the symmetrical structure and symmetrical thermal loading conditions, the model was simplified into the form shown in Fig. 7(b) with only the upper half being studied. The effect of the residual thermal stresses formed in the fabricating process for the functionally graded ceramics is not taken into the calculations.

Because the thermo-mechanical properties (specific heat $c$, thermal conductivity $k$, specific gravity $\rho$, thermal expansion coefficient $\alpha$, Young's modulus $E$ and Poisson's ratio $\nu$) of functionally graded ceramic plate are all variables, i.e. functions of $z$, the calculations of transient temperature fields were carried out by using the perturbation method. The transient thermal stress fields were calculated subsequently by using mechanics of elasticity. Some laws of mixture were employed to calculate the thermo-mechanical properties of $Al_2O_3$–TiC and $Al_2O_3$–(W, Ti)C composites with different mixture ratios, thermal conductivities $k$ and specific heats $c$ obtained by the theory of Kingery,[4] thermal expansion coefficients $\alpha$ obtained by Kerner's equation,[5] and Young's modulus $E$ and Poisson's ratio $v$ obtained by Mori–Tanaka's equation.[6] Besides the dimensionless variable in the thickness direction $\bar{z}$, time $t$ was also normalized into $\tau$ for calculation simplicity. Because of the lengthiness and complexity of the calculations by using the perturbation method, the details are omitted here for brevity.

The temperature distributions of functionally graded ceramics FG-1 and FG-2 under surface cooling (initial

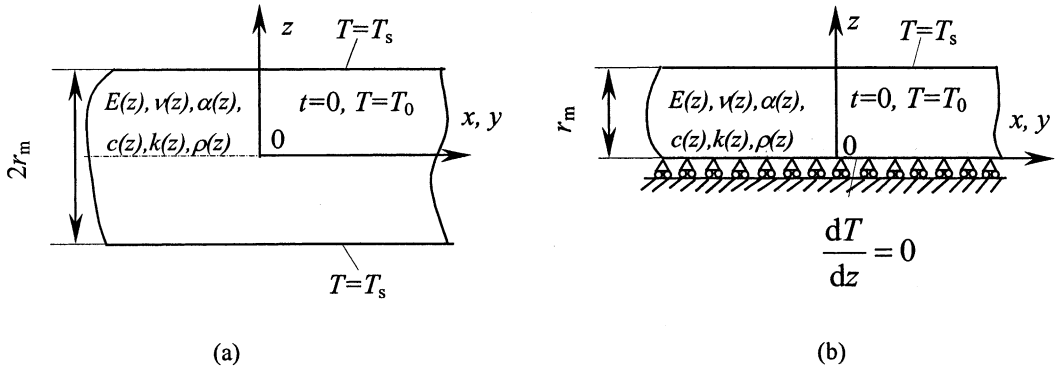


Fig. 7. Functionally graded ceramic plate with symmetrical structure.

temperature $T_0 = 300$ °C and ambient temperature $T_s = 20$ °C) are shown in Fig. 8(a) and (b), respectively. It can be seen that the shorter the dimensionless time τ is, the higher the temperature gradient near the surface is; the longer τ is, the lower the temperature gradient near the surface is.

The calculation results of transient thermal stress distribution under surface cooling (Fig. 9) revealed clearly that the tensile stress generated in the surface region ($\bar{z} = 1.0$), while the middle region ($\bar{z} = 0$) was subjected to compressive stress when the dimensionless time τ was shorter. It also can be seen that the shorter the dimensionless time τ is, the higher the tensile stress in the surface region is; the longer τ is, the lower the tensile stress is. When the dimensionless time τ approaches ∞, namely at the steady state, the residual compressive stress will generate in the surface region ($\bar{z} = \pm 1.0$), while the residual tensile stress will generate in the middle region ($\bar{z} = 0$) for both FG-1 and FG-2 since the thermal expansion coefficient of the surface region is lower than that of the middle region (Table 1).

### 3.4. The effect of the compositional distribution on the thermal shock resistance

In order to investigate the influence of compositional distribution on thermal stress distribution, the unsteady thermal stress distributions of a homogeneous $Al_2O_3$–TiC (30 vol.%$Al_2O_3$ + 70 vol.%TiC) and a homogeneous $Al_2O_3$–(W, Ti)C (55 vol.%$Al_2O_3$ + 45 vol.%(W, Ti)C) ceramic plate under surface cooling (initial temperature $T_0 = 300$ °C and ambient temperature $T_s = 20$ °C) were calculated also by using the same method. The calculation results for $\tau = 0.1$ are listed in Table 2.

It can be seen that the absolute values of both tensile stresses in the surface region and the compressive stresses in the middle region of homogeneous $Al_2O_3$–TiC and $Al_2O_3$–(W, Ti)C ceramic plates are higher than those of FG-1 and FG-2 graded ceramic plates respectively. The similar characteristics of the thermal stress distributions can be found for $\tau = 0.01$ and $\tau = 1.0$.

The lower thermal stresses of the functionally graded ceramic plate should be attributed to both the higher thermal conductivity and the higher thermal expansion

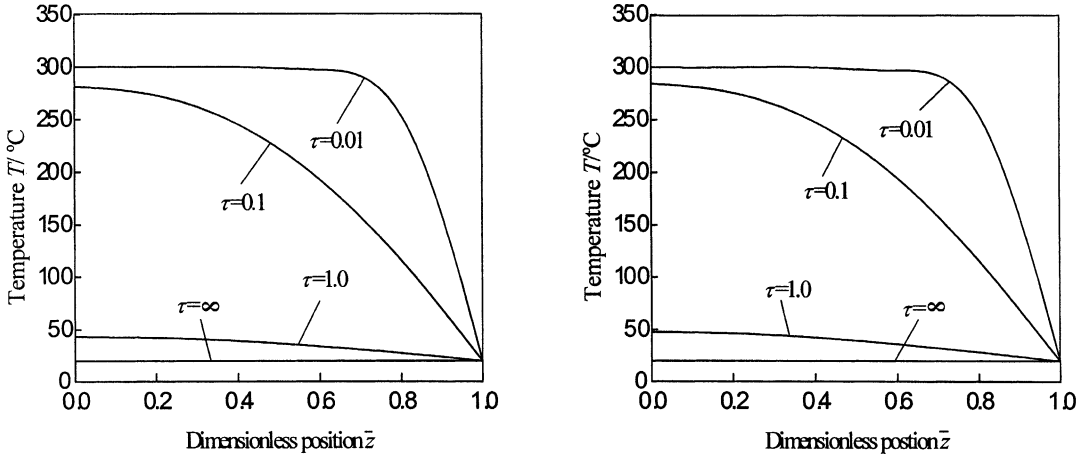


Fig. 8. Temperature distribution under surface cooling.

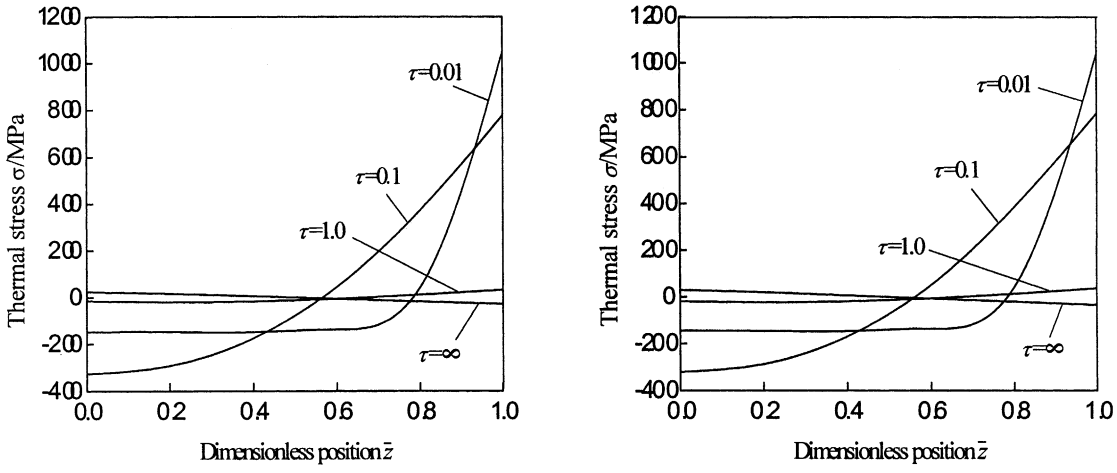


Fig. 9. Thermal stress distribution under surface cooling.

Table 2
Distribution of thermal stress $\sigma(\bar{z}, \tau)$/MPa under surface cooling for $\tau = 0.1$

| Materials | $\bar{z}$ | | | | | |
|---|---|---|---|---|---|---|
| | 0.0 | 0.2 | 0.4 | 0.6 | 0.8 | 1.0 |
| FG-1 plate | −326.3 | −292.0 | −175.7 | 44.5 | 371.1 | 775.9 |
| $Al_2O_3$–TiC plate | −326.9 | −290.8 | −170.7 | 56.5 | 392.5 | 808.5 |
| FG-2 plate | −319.9 | −286.5 | −169.5 | 50.4 | 382.3 | 783.5 |
| $Al_2O_3$–(W,Ti)C plate | −324.6 | −288.7 | −170.4 | 56.1 | 389.7 | 802.7 |

coefficient of the middle region than those of the surface region (Table 1). The former could relax the temperature gradient and the later could partially release the tensile stress in the surface region during the cooling process, and the higher the temperature difference $\Delta T$ $(=T_s - T_0)$ is, the more remarkably the functionally graded ceramic plate release the thermal stress. The lower thermal stress of the functionally graded ceramics than that of homogeneous ceramics under the same thermal shock condition may result in the higher thermal shock resistance in both the increased retained strength and the increased critical temperature difference for the surface cracking.

Furthermore, the higher thermal expansion coefficient of the middle region than that of the surface region leads to the formation of residual compressive stresses in the surface region during the fabricating process. This also contributes to the higher thermal shock resistance of the functionally graded ceramics.

Because the model used in the calculations is an infinite functionally graded ceramic plate with continuous compositional profile, which differs from the bend bars with discrete compositional distribution, this inevitably leads to considerable errors. Also, in virtue of the difficulty in determining the heat transfer coefficient on the surfaces and the difficulty in calculations of transient temperature fields and transient thermal stresses under a convective boundary condition, the time for the surface to attain its maximum thermal stress during a thermal shock process can not be calculated and consequently the critical temperature difference for fracture initiation of the surface layer is very difficult to determine theoretically. So, the above calculations assuming an idealized thermal shock condition (infinitely large heat transfer coefficient on the two surfaces) may also result in errors. Yet the above calculation results can be used as an indirect support for the higher thermal shock resistance of functionally graded ceramics than that of homogeneous ceramics.

## 4. Conclusions

$Al_2O_3$–TiC and $Al_2O_3$–(W, Ti)C functionally graded ceramic tool materials with symmetrical structures, FG-1 and FG-2 were fabricated by using hot pressing technique according to the optimum compositional distribution. The thermal shock resistance of these two graded ceramic materials were evaluated by water quenching and subsequent three-point bending tests of strength diminution. Comparisons were made with the results from parallel experiments conducted using homogeneous $Al_2O_3$–TiC and $Al_2O_3$–(W, Ti)C ceramic tool materials respectively.

Both the critical temperature difference and strength retention properties of thermal shock resistance for the two graded ceramics FG-1 and FG-2 were experimentally found to be higher than those for homogeneous $Al_2O_3$–TiC and $Al_2O_3$–(W, Ti)C cutting ceramics respectively, indicating their increased thermal shock

resistance. The experimental results were supported by the microstructural observations and the calculations of one-dimensional transient temperature fields and transient thermal stress fields in case of surface cooling by using the perturbation method.

## Acknowledgements

This work was supported by the National Natural Science Foundation of China (50105011 and 59505014), the Foundation for the Author of National Excellent Doctoral Dissertation of PR China (200231) and the Scientific Research Foundation for the Returned Overseas Chinese Scholars, State Education Ministry.

## References

1. Swain, M. V., R-curve behavior and thermal shock resistance of ceramics. *J. Am. Ceram. Soc*., 1990, **73**(3), 621–628.
2. Zhao, J., Ai, X., Zhang, J. H. and Huang, C. Z., Design of $Al_2O_3$/TiC functionally graded ceramic tool material. *Chinese Journal of Mechanical Engineering*, 1998, **34**(4), 32–36 (in Chinese).
3. Ai, X., Zhao, J., Huang, C. Z. and Zhang, J. H., Development of an advanced ceramic tool material—functionally graded cutting ceramics. *Materials Science and Engineering A*, 1998, **248**(1-2), 125–131.
4. Kingery, W. D., Bowen, H. K. and Uhlmann, D. R., *Introduction to Ceramics, 2nd edn*. John Wiley & Sons, New York, 1976.
5. Kerner, E. H., The elastic and thermal-elastic properties of composite media. *Proc. Phys. Soc*., 1956, **B69**, 808–813.
6. Mori, T. and Tanaka, K., Average stress in matrix and average elastic energy of materials with misfitting inclusions. *Acta Metall*., 1973, **21**, 571–574.